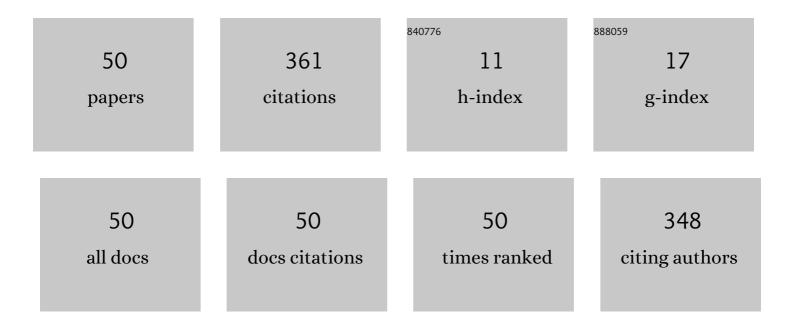
Haoshen Zhu

List of Publications by Year in descending order

Source: https://exaly.com/author-pdf/1423917/publications.pdf Version: 2024-02-01



ΗλΟSHEN 7ΗΠ

#	Article	IF	CITATIONS
1	Bandpass Filter With Ultra-Wide Upper Stopband on GaAs IPD Technology. IEEE Transactions on Circuits and Systems II: Express Briefs, 2022, 69, 389-393.	3.0	7
2	A 28 GHz GaN HEMT quasiâ€circulator with high isolation and high powerâ€handling capability. Microwave and Optical Technology Letters, 2022, 64, 72-76.	1.4	1
3	A 7.2–27.3 GHz CMOS LNA With 3.51 ±0.21 dB Noise Figure Using Multistage Noise Matching Technique. IEEE Transactions on Microwave Theory and Techniques, 2022, 70, 74-84.	4.6	21
4	A wideâ€band balancedâ€ŧoâ€unbalanced power divider using microstripâ€slotlineâ€5IW transitions. Microwave and Optical Technology Letters, 2022, 64, 110-116.	1.4	2
5	A Ka-Band High-Power Switchable Filtering Power Combiner MMIC in 100-nm GaN-on-Si. IEEE Transactions on Industrial Electronics, 2022, 69, 10467-10477.	7.9	2
6	Odd-Element Half-Wave-Rectification Superposition Technique for High-Multiplication Factor Frequency Multipliers Design. IEEE Transactions on Circuits and Systems I: Regular Papers, 2022, 69, 1871-1882.	5.4	3
7	A Simplified Vector-Sum Phase Shifter Topology With Low Noise Figure and High Voltage Gain. IEEE Transactions on Very Large Scale Integration (VLSI) Systems, 2022, , 1-9.	3.1	3
8	Novel Wideband Bandpass Filters Using Double-Sided Quasi-SSPPs Transmission Line. IEEE Transactions on Circuits and Systems II: Express Briefs, 2022, 69, 3174-3178.	3.0	5
9	A 22.2-GHz Injection-Locked Frequency Tripler Featuring Dual Injection and 39.4% Locking Range. IEEE Transactions on Microwave Theory and Techniques, 2022, 70, 3548-3556.	4.6	2
10	A Millimeter-Wave Variable-Gain Power Amplifier With Pâ,•dB Improvement Technique in 65-nm CMOS. IEEE Microwave and Wireless Components Letters, 2022, 32, 1427-1430.	3.2	1
11	A Novel Piezoresistive Transducer for Bulk Mode MEMS Resonator. , 2022, , .		0
12	High Performance Balanced Bandpass Filters With Wideband Common Mode Suppression. IEEE Transactions on Circuits and Systems II: Express Briefs, 2021, 68, 1897-1901.	3.0	18
13	A wideband filtering microstripâ€toâ€microstrip vialess vertical transition on <scp>CPW MMR</scp> . International Journal of RF and Microwave Computer-Aided Engineering, 2021, 31, e22567.	1.2	2
14	Compact balanced bandpass filter based on dualâ€sided parallelâ€strip line. International Journal of RF and Microwave Computer-Aided Engineering, 2021, 31, e22586.	1.2	1
15	A 9.8–30.1 GHz CMOS low-noise amplifier with a 3.2-dB noise figure using inductor- and transformer-based gm-boosting techniques. Frontiers of Information Technology and Electronic Engineering, 2021, 22, 586-598.	2.6	3
16	A CMOS Low-Power Variable-Gain LNA Based on Triple Cascoded Common-Source Amplifiers and Forward-Body-Bias Technology. , 2021, , .		3
17	A transformerâ€based injectionâ€locked frequency divider. Microwave and Optical Technology Letters, 2021, 63, 2565-2569.	1.4	0
18	A New Class of Wideband MS-to-MS Vialess Vertical Transition With Function of Filtering Performance. IEEE Transactions on Circuits and Systems II: Express Briefs, 2021, 68, 1877-1881.	3.0	3

HAOSHEN ZHU

#	Article	IF	CITATIONS
19	Analytical Design of Millimeter-Wave 100-nm GaN-on-Si MMIC Switches Using FET-Based Resonators and Coupling Matrix Method. IEEE Transactions on Microwave Theory and Techniques, 2021, 69, 3307-3318.	4.6	11
20	A Wideband CMOS LNA Using Transformer-Based Input Matching and Pole-Tuning Technique. IEEE Transactions on Microwave Theory and Techniques, 2021, 69, 3335-3347.	4.6	29
21	A 15–38 GHz Vector-Summing Phase-Shifter With 360° Phase-Shifting Range Using Improved I/Q Generator. IEEE Transactions on Circuits and Systems II: Express Briefs, 2021, 68, 3199-3203.	3.0	10
22	A 3.5GHz CMOS Transceiver for Sub-6GHz and Mm-Wave Co-Existed 5G Communication Systems. , 2021, , .		1
23	Limits to Thermal-Piezoresistive Cooling in Silicon Micromechanical Resonators. Journal of Microelectromechanical Systems, 2020, 29, 677-684.	2.5	1
24	A PLL Synthesizer for 5G mmW Transceiver. , 2020, , .		1
25	A Wideband 7.5-29.5 GHz LNA with Constant NF by Using Multistage Noise Matching at High Frequencies. , 2020, , .		2
26	Compact Balanced Bandpass Filter With Wideband Common Mode Suppression. , 2020, , .		3
27	A 21-41 GHz Compact Wideband Low-Noise Amplifier Based on Transformer-Feedback Technique in 65-nm CMOS. , 2020, , .		1
28	A 24-30GHz Asymmetric SPDT Switch for 5G Millimeter-Wave Front-End. , 2020, , .		4
29	A 24-30GHz GaN-on-Si Variable Gain Low-Noise Amplifier MMIC. , 2020, , .		2
30	A Broadband dB-linear VGA with third-order interleaving active feedback. , 2020, , .		0
31	A Wideband LNA Based on Current-Reused CS-CS Topology and Gm-boosting Technique for 5G Application. , 2019, , .		12
32	Thermal-Piezoresistive Tuning of the Effective Quality Factor of a Micromechanical Resonator. Physical Review Applied, 2018, 10, .	3.8	14
33	Non-Reciprocal Acoustic Transmission in a GaN Delay Line Using the Acoustoelectric Effect. IEEE Electron Device Letters, 2017, 38, 802-805.	3.9	22
34	Switchable Lamb wave delay lines using AlGaN/GaN heterostructure. , 2017, , .		4
35	Lamb wave dispersion in gallium nitride micromechanical resonators. , 2016, , .		2
36	Phase Noise Reduction in a VHF MEMS-CMOS Oscillator Using Phononic Crystals. IEEE Journal of the Electron Devices Society, 2016, 4, 149-154.	2.1	11

HAOSHEN ZHU

#	Article	IF	CITATIONS
37	Design of Phononic Crystal Tethers for Frequency-selective Quality Factor Enhancement in AlN Piezoelectric-on-silicon Resonators. Procedia Engineering, 2015, 120, 516-519.	1.2	25
38	Piezoresistive Transduction in a Double-Ended Tuning Fork SOI MEMS Resonator for Enhanced Linear Electrical Performance. IEEE Transactions on Electron Devices, 2015, 62, 1596-1602.	3.0	11
39	Piezoresistive Readout Mechanically Coupled Lamé Mode SOI Resonator With \$Q\$ of a Million. Journal of Microelectromechanical Systems, 2015, 24, 771-780.	2.5	22
40	Dependence of temperature coefficient of frequency (TCf) on crystallography and eigenmode in N-doped silicon contour mode micromechanical resonators. Sensors and Actuators A: Physical, 2014, 215, 189-196.	4.1	17
41	Differential-capacitive-input and differential-piezoresistive-output enhanced transduction of a silicon bulk-mode microelectromechanical resonator. Sensors and Actuators A: Physical, 2014, 210, 41-50.	4.1	12
42	Active electronic cancellation of nonlinearity in a High-Q longitudinal-mode silicon resonator by current biasing. , 2014, , .		4
43	Diameter dependence of electron mobility in InGaAs nanowires. Applied Physics Letters, 2013, 102, .	3.3	31
44	Material nonlinearity limits on a Lamé-mode single crystal bulk resonator. , 2012, , .		2
45	Benchmarking the passive differential input technique to shielded GSG probes. , 2012, , .		0
46	Critical components in 140 GHz communication systems. , 2012, , .		2
47	Reversed Nonlinear Oscillations in Lamé-Mode Single-Crystal-Silicon Microresonators. IEEE Electron Device Letters, 2012, 33, 1492-1494.	3.9	10
48	System-level circuit simulation of nonlinearity in micromechanical resonators. Sensors and Actuators A: Physical, 2012, 186, 15-20.	4.1	15
49	Simulating Nonlinearity in MEMS Resonators by a Charge Controlled Capacitor. Procedia Engineering, 2011, 25, 403-406.	1.2	3
50	Direct Parameter Extraction for Piezoresistively-sensed MEMS Resonators Embedded in Parasitic Capacitive Feedthrough. Procedia Engineering, 2011, 25, 515-518.	1.2	0